RESEARCH ARTICLE

The Mitochondrial Unfolded Protein Response Protects against Anoxia in *Caenorhabditis elegans*

Salvador Peña[1], Teresa Sherman[2], Paul S. Brookes[3,4], Keith Nehrke[2,4]*

1 Department of Pathology and Laboratory Medicine, University of Rochester Medical Center, Rochester, New York, United States of America, 2 Department of Medicine, University of Rochester Medical Center, Rochester, New York, United States of America, 3 Department of Anesthesiology, University of Rochester Medical Center, Rochester, New York, United States of America, 4 Department of Pharmacology and Physiology, University of Rochester Medical Center, Rochester, New York, United States of America

* keith_nehrke@urmc.rochester.edu

Abstract

The mitochondrial unfolded protein response (UPR^mt) is a surveillance pathway that defends proteostasis in the "powerhouse" of the cell. Activation of the UPR^mt protects against stresses imposed by reactive oxygen species, respiratory chain deficits, and pathologic bacteria. Consistent with the UPR^mt's role in adaption, we found that either its pharmacological or genetic activation by ethidium bromide (EtBr) or RNAi of the mitochondrial AAA-protease *spg-7* was sufficient to reduce death in an anoxia-based *Caenorhabditis elegans* model of ischemia-reperfusion injury. The UPR^mt-specific transcription factor *atfs-1* was necessary for protection and *atfs-1* gain-of-function (gf) mutants were endogenously protected from both death and dysfunction. Neurons exhibited less axonal degeneration following non-lethal anoxia-reperfusion (A-R) when the UPR^mt was pre-activated, and consistent with the concept of mitochondrial stress leading to cell non-autonomous (ie. "remote") effects, we found that restricted activation of the UPR^mt in neurons decreased A-R death. However, expression of the *atfs-1(gf)* mutant in neurons, which resulted in a robust activation of a neuronal UPR^mt, did not upregulate the UPR^mt in distal tissues, nor did it protect the worms from A-R toxicity. These findings suggest that remote signaling requires additional component(s) acting downstream of *de facto* mitochondrial stress.

Introduction

The mitochondrial unfolded protein response (UPR^mt) is an adaptive signaling pathway that was first identified in mammals [1], but has been best characterized genetically in the nematode *Caenorhabditis elegans* [2–5]. Misfolded proteins in the mitochondria trigger the expression of a repertoire of genes that relieve respiratory burden and restore proteostasis (for review, see reference [6]). Activation of the UPR^mt occurs in response to disruptions in the stoichiometric equilibrium between nuclear and mitochondria-encoded electron transport chain (ETC)

subunits [7], reactive oxygen species (ROS) [8, 9], and by exposure to pathogenic bacteria [10], suggesting that it is part of a surveillance mechanism that responds to disruption of core physiologic processes [8, 10–13]. Interestingly, mitochondrial stress in *C. elegans* neurons has been shown to activate the UPR^{mt} in distal tissues and to regulate lifespan, leading to the idea that mitochondrial proteostasis is a sounding board that can trigger adaptation remotely through cell-cell communication [14].

In *C. elegans*, mito-nuclear retrograde signaling via the bZip transcription factor, ATFS-1, is a critical component of the UPR^{mt} axis [15, 16]. ATFS-1 normally traffics to mitochondria, however during mitochondrial dysfunction a fraction of ATFS-1 fails to reach the mitochondria and instead accumulates in the nucleus. Additionally, the UPR^{mt} is regulated by dimerization and nuclear localization of the *dve-1* encoded transcription factor along with a small ubiquitin like protein *ubl-5*, as well as the activity of mTOR regulator, *rheb-1*. [2, 3]. Importantly, ATFS-1 coordinates mito-nuclear genomic output to properly balance the stoichiometry of electron transport chain complex assembly in order to maintain oxidative phosphorylation during mitochondrial stress [15]. Several mitochondrial electron transport chain (ETC) mutants show UPR^{mt} activation and require *atfs-1* for survival [16] suggesting that this signaling pathway helps the organism to cope with mitochondrial dysfunction.

In the cellular stress imposed by oxygen deprivation, mitochondria are central to both death and survival (for review, see reference [17]). Significant events leading to death are irreversible inhibition of oxidative phosphorylation, proton leak across the mitochondrial inner membrane, calcium overload, reactive oxygen species (ROS) generation and permeability transition pore opening [18–23]. However, interventions that preserve mitochondria function, for example by scavenging ROS or inhibiting PT pore opening, are protective [24–26].

Recently, anoxia-reperfusion (A-R) has been shown to cause the accumulation of misfolded proteins in the mitochondria of *C. elegans* [27]. A-R has been used extensively as a surrogate for ischemia-reperfusion in worms, due to their diminished sensitivity to low oxygen levels compared to mammals [28]. Protecting the mitochondrial protein folding environment by simply over expressing mitochondrial molecular chaperones (Hsp-60 and mtHsp-70) can protect mammalian cells from ischemia-reperfusion (I-R) injury [29, 30] and inhibiting mitochondrial translation through knockdown of aminoacyl-tRNAs has been shown to protect against A-R injury in worms [31]. Collectively, it seems that interventions that support mitochondrial proteostasis can protect against the detrimental effects of low oxygen. In fact, pre-activation of the UPR^{mt} was recently shown to protect against anoxia in worms [27].

Herein, we build on the foundation that *atfs-1* is required for protection from A-R injury, to show that *atfs-1* gain-of-function (gf) mutants that exhibit constitutive activation of the UPR^{mt} are endogenously protected. Based on this result, we hypothesized that protection might occur through intrinsic, cell autonomous processes or through remote effects that are coordinated throughout the organism (ie, "mitokine" signaling). To address this idea, we developed of a novel genetic model for single-copy cell restricted expression of an *atfs-1(gf)* mutant. Our results indicate that cell autonomous protection from A-R injury can be elicited through an *atfs-1(gf)*, but that remote UPR^{mt} activation and protection from death may require other pathway(s) that responds to *de facto* mitochondrial stress.

Materials and Methods

Strains

Worm strains were routinely propagated using standard culture techniques at 20°C on nematode growth media (NGM) agar plates containing 5 μg/ml cholesterol and seeded with OP50 bacteria, as described [32]. The strains used in this work are:

SJ4058, zcIs9 [*Phsp-60::GFP*] V; CMH5, *atfs-1(tm4525)* V; QC115, *atfs-1(et15)* V; EG4322, ttTi5605 II; *unc-119(ed9)* III;; KWN176, rnyIs13 [*Pmec-4::mCherry; unc-119(+)*] X; KWN 456, rnySi37 [*Patfs-1::wCherry::atfs-1::GFP, cb-unc-119(+)*] II; KWN 495, *pha-1 (e2123ts)* III, *him-5 (e1490)* V, rnyEx289 [*Patfs-1::flp, Pmyo-2::mCherry, pha-1(+)*]; KWN484, *atfs-1(tm4525)* V, rnySi37, zcIs9, rnyEx289; KWN525 rnySi49 [*Patfs-1::wCherry::atfs-1(et15)::GFP, cb-unc-119 (+)*] II; *unc-119(ed3)* III; KWN529, *pha-1 (e2123ts)* III, *him-5 (e1490)* V, rnyEx297 [*Prab-3::flp, Pmyo-2::mCherry, pha-1(+)*]; KWN566, rnyIs13, zcIs9; KWN567, *atfs-1(tm4525)*, rnyIs13, zcIs9; KWN568, *atfs-1(et15)*, rnyIs13, zcIs9; KWN562, *atfs-1(tm4525)*, rnySi49, zcIs9, rnyEx297; KWN569, rnySi49, zcIs9, rnyEx297; KWN591, *atfs-1(tm4525)*, rnySi49, zcIs9, rnyIs013, rnyEx289; KWN590, rnySi49, zcIs9, rnyIs013, rnyEx289; HC196, *sid-1(qt9)*; AGD724, *sid-1(qt9)*, uthIs243 [*Prab-3::cco-1HP, Pmyo-2::tdTomato*]

Standard genetic protocols were used for crosses. The zcIs9 insertion on chromosome V is closely linked to *atfs-1*. Hence, GFP signal was used to follow *atfs-1* following mating. To confirm that the genomic *atfs-1* allele co-segregated with zcIs9, the final strains were PCR genotyped using primers 5′-GCCTCCTTTCGCCTTTTGTCATC-3′, 5′-GCACAGCTTCTCCGATTCAGTG-3′, and 5′-gggggatttttagtcggcaatg-3′. These primers do not amplify the chromosome II MosSCI insertions. PCR products were sequenced to identify the *atfs-1 (et15)* allele, which is a missense mutation. MosSCI insertions were confirmed using primers OG967, 5′-AGGCAGAATGTGAACAAGACTCG-3′ and OG970, 5′-ATCGGGAGGCGAACCT AACTG-3′, as described [33].

Molecular Biology

The *atfs-1* promoter (~2.5 kb) was PCR amplified from genomic DNA using primers 5′-ACA CGTCGACCAAACAATTTGATGGTACTGTTTCAGAT-3' and 5'-ACACCCTAGGCGAAGTTAC ACCTGCAAATGTACAAG-3' and cloned into pFH6.II-linker [34] as an *Avr*II-*Sal*I fragment to create pSEP1. The 3' untranslated region from *atfs-1* was PCR amplified from genomic DNA using primers 5′-ACACGCGGCCGCCAATAATCAGAATTCGAAACAATTGTTC-3′ and 5′-ACACACTAGTCCTAGGTTGGCTAAACAGGTAACG-3′ and inserted into pSEP1 as a *Not*I-*Spe*I fragment to create pSEP2. A *Sal*I-*Acc*65I FRT-wCherry-FRT fragment was cloned from pWD176-myo-2-flop-wCherry [9] into pSEP2 to create pSEP3. The *atfs-1* open reading frame was PCR amplified from wild-type genomic DNA with primers 5′-ACACGGTACCAAAAATG TTTTCCCGTGTGGGACGTCTC-3′ and 5′-ACACGGTACCTGAATAATGGCGCCCATTTTACG AAG-3′ and inserted into pSEP3 as an *Acc*65I fragment to create pSEP4. The *atfs-1(et15)* open reading frame was PCR amplified using identical primers and inserted into pSEP3 to create pSEP6. pSEP4 and pSEP6 were digested with *Avr*II-*Spe*I and cloned into the *Spe*I site in the MosSCI vector pCFJ151-p5605 [33] to create pSEP5 and pSEP7, respectively. The *Age*I-*Avr*II fragment from pWD79-hsp-2u-flp-RV (obtained courtesy of Dr. Wayne Davies) was cloned into the *Age*I-*Spe*I sites of pFH6.II in place of GFP to create pFLF1. The *rab-3* promoter was PCR amplified from genomic DNA using primers 5′-ATATGTCGACCAGCCGCAATCTGAAA ATAGGGCTACTGTAG-3′ and 5′-ATATCCTAGGGACGACGACGACCTCGACGG-3′ and cloned into pFLF1 as a *Sal*I-*Avr*lI fragment to create pSEP10. The *atfs-1* promoter was also cloned into pFLF1 to create pSEP11. All PCR-amplified fragments were sequenced to verify fidelity.

Transgenesis and MosSCI Single Copy Gene Insertion

Injection of DNA into the gonads of young adult animals was performed as described [35]. The protocol for single copy insertion has been similarly well described [33, 36]. Briefly, a strain containing the Mos transposon ttTi6505 in chromosome II was injected with pSEP5 or

pSEP7, along with vectors coding for positive and negative selectable markers and an inducible Mos transposase. Following recombination between pSEP5 or pSEP7 and the ttTi5605 site, the chromosome II integration locus was PCR amplified and sequenced to confirm the presence of a full-length insert. All resulting strains were backcrossed to wildtype N2 prior to use.

Anoxia-Reperfusion

Developmentally-synchronized populations of hermaphrodites were established by using alkaline-bleach treatment (20% commercial bleach, 500 mM NaOH) to generate embryos from gravid adults. These embryos were then cultured under standard conditions at 20°C until adulthood, which was defined as 1 day after vulva development was complete, then subject to anoxia. For experiments examining axonal degeneration, staged L1/L2 larvae (24 hours post-hatch) were used in place of adults. Experimental anoxia was established as described [37]. Briefly, the worms were washed 3x in M9 solution (22 mM KH_2PO_4, 42 mM Na_2HPO_4, 86 mM NaCl, 1mM $MgSO_4$, pH 7) and transferred to an anaerobic chamber (Coy Lab Products, USA) equipped with a palladium catalyst to scavenge oxygen ($O_2 < 0.01$ ppm) for 20 h under 95% N_2 and 5% H_2 at ~26°C. Worms were scored for viability 20–24 hours after anoxic exposure as previously described [38]. In general, 2–6 replicates (or individual plates) were assayed per day per condition. The percentage lethality from each plate was then averaged to create a single data point, representing from 49–946 worms (average of 223 worms per data point; see S1 Table for raw data). Experimental manipulations were always assessed in parallel with controls, in order to normalize to index lethality, which fluctuated on a daily basis and was the greatest source of experimental variability. For presentation purposes, the values from individual paired trials were plotted side-by-side, together with their averages.

RNA Interference

Synchronized larval stage 2/3 worms were moved to plates supplemented with transformed HT115 E.coli bacteria where an *spg-7* insert flanked by T7 promoter sites or empty vector control (pPD129.36) was induced using IPTG. Worms were incubated on these plates for at least 24 hours prior to experimental use.

Imaging

Worms were imaged on a 2% agarose pad under anesthetic (0.1% tetramisole). Neuronal puncta were visualized from transgenic worms expressing a red mCherry fusion in mechanosensory neurons, in the L2–L3 stage as previously described [39], using a Nikon Eclipse TE2000-U microscope (Nikon USA, Melville, NY, USA) with a Polychrome V monochromator (TILL Photonics, Gräfelfing, Germany) running TILLvisION software. Neuronal cell bodies were identified under a Texas Red filter set using a 10x objective, then viewed at higher magnification, typically with a 100x oil objective, to assess axonal breaks and abnormalities. Most of these consisted of puncta where the neuronal process was visibly enlarged and at least 2-fold more fluorescent than the surrounding process. The number of abnormalities in either the PVML or PVMR, one of two mechanosensory neurons in the posterior of the worm, was scored in a region extending from the cell body to the vulva. These processes under normal conditions are extremely homogenous with respect to the distribution of fluorescent reporter. Since they run close to the surface or "skin" of the worm, they are easily scored. In general, ten worms were analyzed per day, the data was averaged, and the experiments were repeated 3–4 times (see S1 Table for raw data). Other strains expressing various gene fusions, reporters, or fluorescent markers were examined using an Olympus FV1000 confocal microscope (available as part of the University of Rochester Confocal Core) under appropriate illumination.

Statistics

Statistical significance was determined through Student's *t* tests, comparing paired trials. "N" refers to the number of trials (and hence paired experimental replicates) analyzed, each consisting of > twenty worms.

Results

Mitochondria are pivotal for determining survival following exposure to low oxygen levels, and ROS generated under these conditions can lead to both damage and adaptation. Worms are resistant to hypoxia [28] and hence A-R has been utilized to simulate I-R in this genetic model organism [38, 40]. In addition, worms are normally cultivated from 15–25°C and the A-R model utilizes a modestly elevated temperature (26°C) to sensitize the worms to anoxic toxicity. Hence, it is possible that interventions that modulate A-R toxicity may have their basis in thermal tolerance. However, this is true in mammalian systems, as well, where I-R injury is also temperature sensitive, and there is a large body of evidence suggesting that A-R translates well as a surrogate for I-R in mammalian cells (for review, see reference [41]). Here, we utilized *C. elegans* to determine the influence of UPR^{mt} activation on surviving A-R.

The UPR^{mt} reporter P*hsp-60::GFP* is strongly activated by RNAi mediated knockdown of *spg-7* (*spg-7(RNAi)*), a mitochondrial quality control m-AAA protease (Fig 1A). *A priori* treatment with *spg-7*(RNAi) reduced death following A-R (vector control 71 ± 7%; *spg-7(RNAi)* 49 ± 8%, error is SEM, p = 0.02; Fig 1D), as did 30 mcg/mL EtBr, an established chemical activator of the UPR^{mt} (S1 Fig). Protection elicited from both regiments was lost in the *atfs-1 (tm4525)* loss-of-function (lf) mutant (*atfs-1(tm4525)* 58 ± 14%; *spg-7(RNAi)* 73 ± 11%; error is SEM, p = 0.14; Fig 1E).

Next we examined whether activation of *atfs-1* is sufficient for protection. We took advantage of forward genetic screen for mutations that protected against the toxic non-cholesterol effects of statins [42]. The *atfs-1(et15)* gf allele contains a missense mutation in the first six amino acids that is predicted to reduce ATFS-1 mitochondrial import, and the resulting activation of the UPR^{mt} was shown to protect against statin toxicity [42]. As expected, *atfs-1(et15)* mutants exhibited constitutive induction of the UPR^{mt} reporter gene *hsp-60* (Fig 1C). The *atfs-1(et15)* mutants also exhibited decreased death following A-R (wildtype 80 ± 7%; *atfs-1(et15)* 36 ± 10%, error is SEM, p = 0.006; Fig 1F).

We then determined whether induction of the UPR^{mt} could protect tissues from sub-lethal A-R injury. The fluorescent reporter mCherry was expressed in mechanosensory neurons under control of the *mec-4* promoter in order to measure axonal damage [43] (Fig 2A). Process abnormalities including breaks and "bead-on-a-string" type puncta (Fig 2B) have been reported to occur following A-R in these neurons [38]. Following A-R in young larva, which are less susceptible to A-R than adults and hence were used here as a sub-lethal model, *atfs-1 (gf)* mutants formed fewer axonal puncta than control animals (wildtype 2.4 ± 0.6; *atfs-1(et15)* 1.4 ± 0.3, error is SD, p = 0.02; Fig 2C). While the difference in puncta between genotypes was small, which is expected given the nature of the model, the data is robust and the difference statistically significant. Previous reports have suggested that upwards of 10 puncta may form following A-R [38]; however, in our hand the only worms that exhibited this many abnormalities were dead or close to death and hence unsuitable for analysis. It is also possible that the differences we observe are due to labeling with mCherry rather than GFP, as was used previously [38].

Neuronal mitochondrial stress can be sensed remotely, suggesting that cells are able to coordinate adaptive responses based upon communicating the status of their mitochondria (Fig 3A) [14]. We found that a small hairpin loop RNA that targets complex IV (*cco-1*HP)
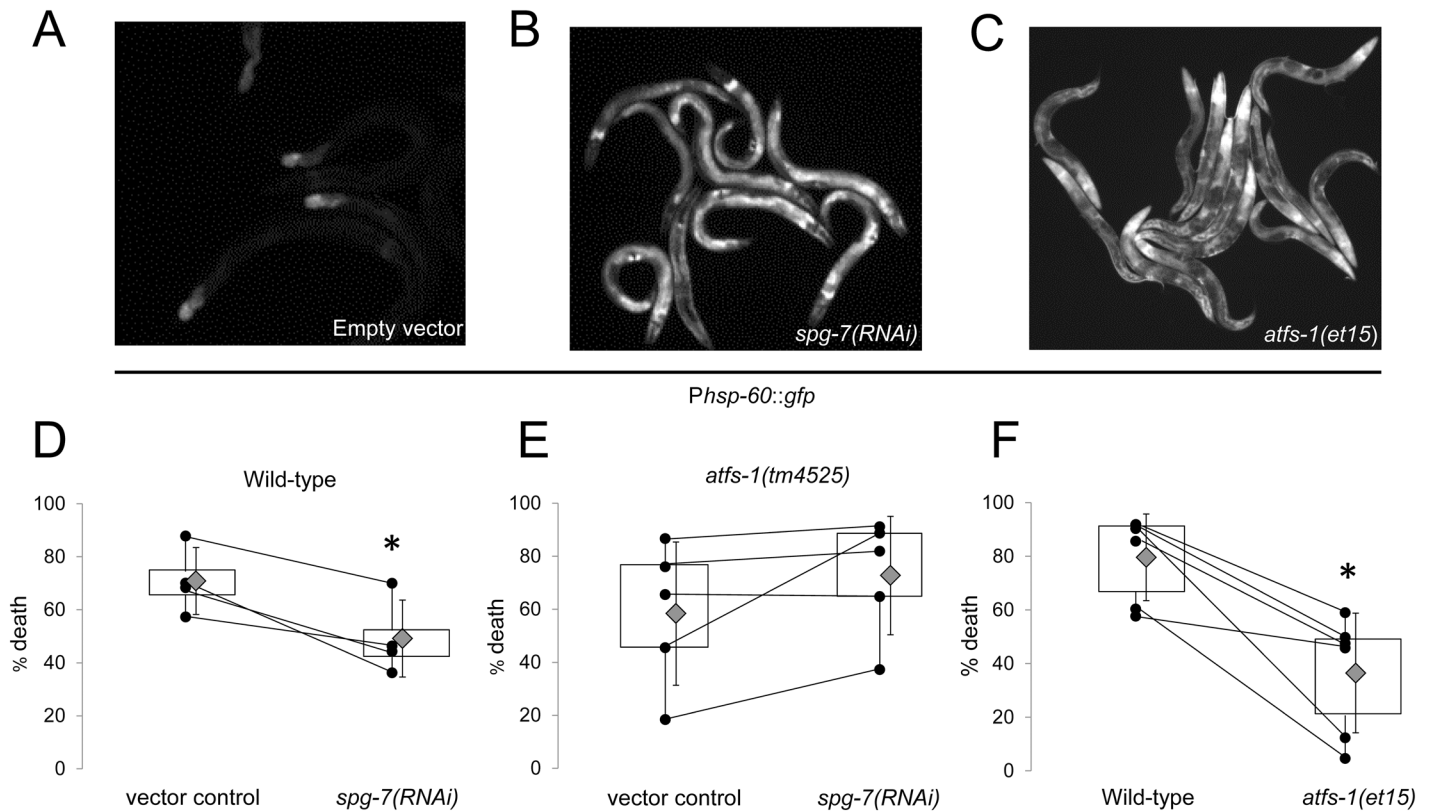
Fig 1. *Atfs-1* is both necessary and sufficient for UPRmt activation and reduced death from anoxia-reperfusion. Representative fluorescent photomicrographs of P*hsp60*::*GFP* activation in A.) vector control and B.) UPRmt inducer *spg-7(RNAi)* treated worms and in C.) an *atfs-1(et15)* gain-of-function mutant. D.) Box-and-whisker plot showing that pre-induction of the UPRmt with *spg-7(RNAi)* reduces death following A-R (n = 4, p*[Student's t test] <0.05). E.) Box-and-whisker plot showing that *spg-7(RNAi)* does not protect *atfs-1(tm4525)* loss-of-function worms from A-R toxicity (n = 5, p* [Student's t test] <0.05). F.) Box-and-whisker plot showing that *atfs-1(et15)* mutants are constitutively less susceptible to A-R (n = 6, p*[Student's t test] <0.05). Experimental replicates are shown as black dots; lines between replicates indicate that they were run on the same day. Grey diamonds are means with the error shown as standard deviations.

doi:10.1371/journal.pone.0159989.g001
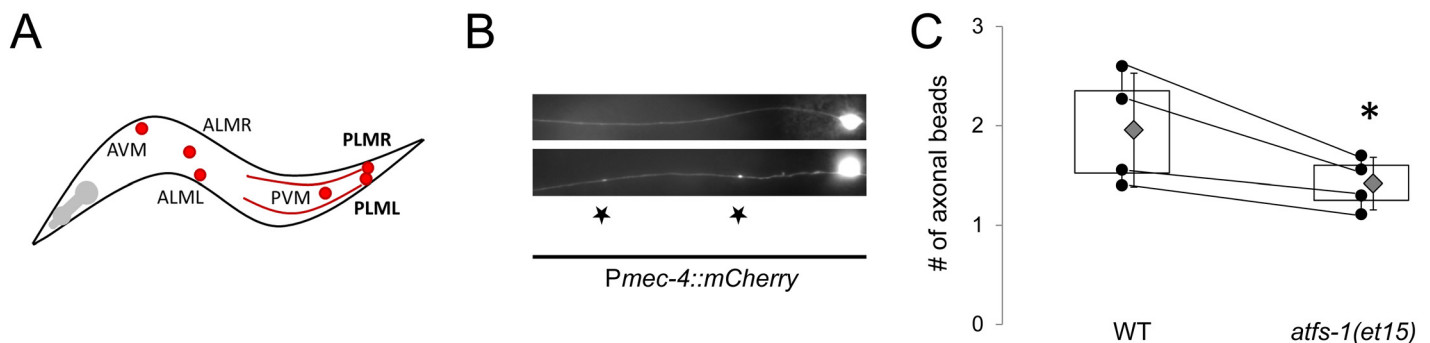
Fig 2. A gain-of-function in *atfs-1* attenuates axonal degeneration following anoxia-reperfusion. A.) Schematic representation of mechanosensory neurons (red dots indicate soma) in the worm, and the PLM axonal processes that were used to measure degeneration. B.) Representative fluorescent photomicrograph of an integrated P*mec-4*::*mCherry* reporter in wildtype worms (top image) and following A-R (bottom image). Scored puncta are denoted by stars. C.) *atfs-1(et15)* worms develop fewer puncta following A-R (n = 4 independent trials with ~10 worms per genotype per trial), p*[Student's t test] <0.05). The error is the standard deviation.
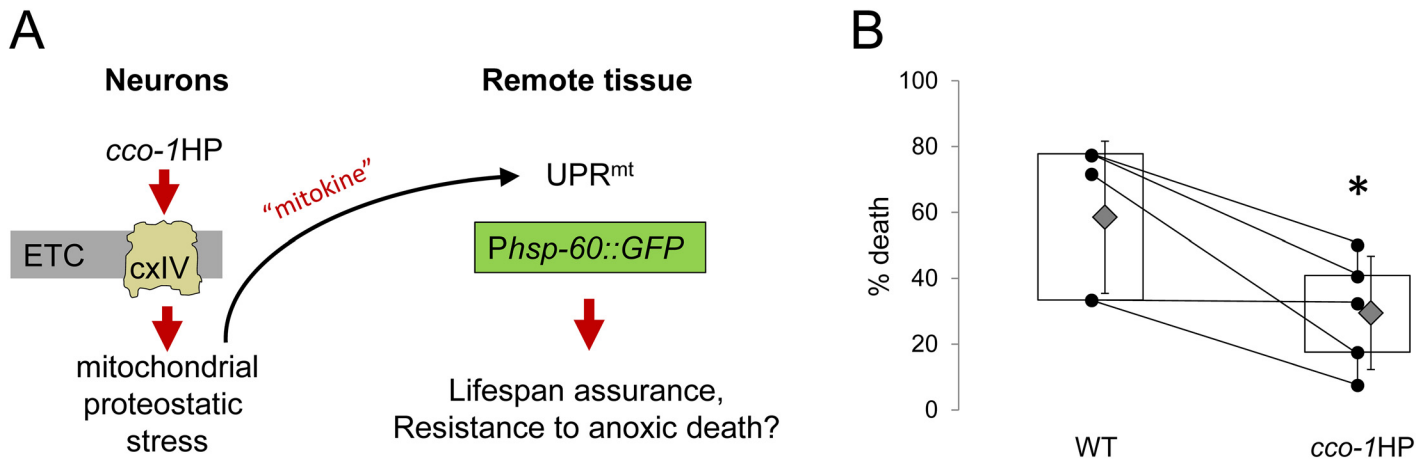
doi:10.1371/journal.pone.0159989.g002

Fig 3. Electron transport chain dysfunction in neurons reduces anoxia-reperfusion toxicity. A.) Schematic of how *cco-1*HP interference with Complex IV leads to mitochondrial stress in neurons, which is transduced remotely through an unidentified "mitokine" to elicit adaptive signaling measures in distal cells. B.) Box-and-whisker plot showing that neuronal *cco-1*HP reduces death following A-R (n = 5, p*[Student's t test] <0.05). Experimental replicates are shown as black dots; lines between replicates indicate that they were run on the same day. Grey diamonds are means with the error shown as standard deviations.

expressed under the control of the pan-neuronal *rab-3* promoter decreased A-R death (wild-type 59 ± 12%; *cco-1*HP 30 ± 9%, error is SEM, p = 0.03; Fig 3B). This suggests that neurons are able to coordinate remote adaptation among the whole organism in response to intrinsic mitochondrial stress. However, the *cco-1*HP model presumably combines *de facto* mitochondrial proteotoxicity through ROS generation with compensatory activation of the UPR^{mt}. As such, we were motivated to ask whether neuronal expression of the *atfs-1(gf)* mutant, which exhibits compensation in the absence of stress, would also increase survival.

To achieve this, we generated a novel genetic system that combines two techniques for restricting gene expression. Transgenesis in worms is generally achieved through multi-copy extra-chromosomal arrays that drive recombinant expression. However, the UPR^{mt} reflects a balance between mitochondrial and nuclear ATFS-1 targeting, which is likely to be prone to overexpression artifacts. Moreover, cell-specific promoters exhibit a range of temporal and quantitative differences in expression levels. To circumvent these issues, we first generated a genetic model where FLP recombinase is used to activate gene expression [44]. A recombinant *atfs-1* transgene was cloned where the promoter is interrupted by a *wCherry* insert that is itself flanked by FLP recombinase sites (Fig 4A). This transgene was then integrated via Mos-mediated single copy gene insertion (MosSCI) into the ttTi5605 site on chromosome II [33]. Hence, transgenic ATFS-1 expression should occur at physiological levels from its own promoter but only in a subset of tissues defined by the overlap with a promoter chosen to drive recombinant FLP expression.

Under basal conditions in the absence of FLP recombinase, *wCherry* was widely expressed at low levels (long exposure, Fig 4B), suggesting that the *atfs-1* promoter was active. When the MosSCI *atfs-1(+)* transgene was placed into a genomic *atfs-1(lf)* background, the worms were unable to activate the UPR^{mt} P*hsp-60*::*GFP* reporter in response to *spg-7(RNAi)* (Fig 4C), suggesting effective suppression of ATFS-1 expression by the *wCherry* promoter interruption. In contrast, expression of FLP recombinase from the *atfs-1* promoter itself restored the ability to activate the UPR^{mt} P*hsp-60*::*GFP* reporter (Fig 4C), suggesting effective de-suppression through *wCherry* excision.
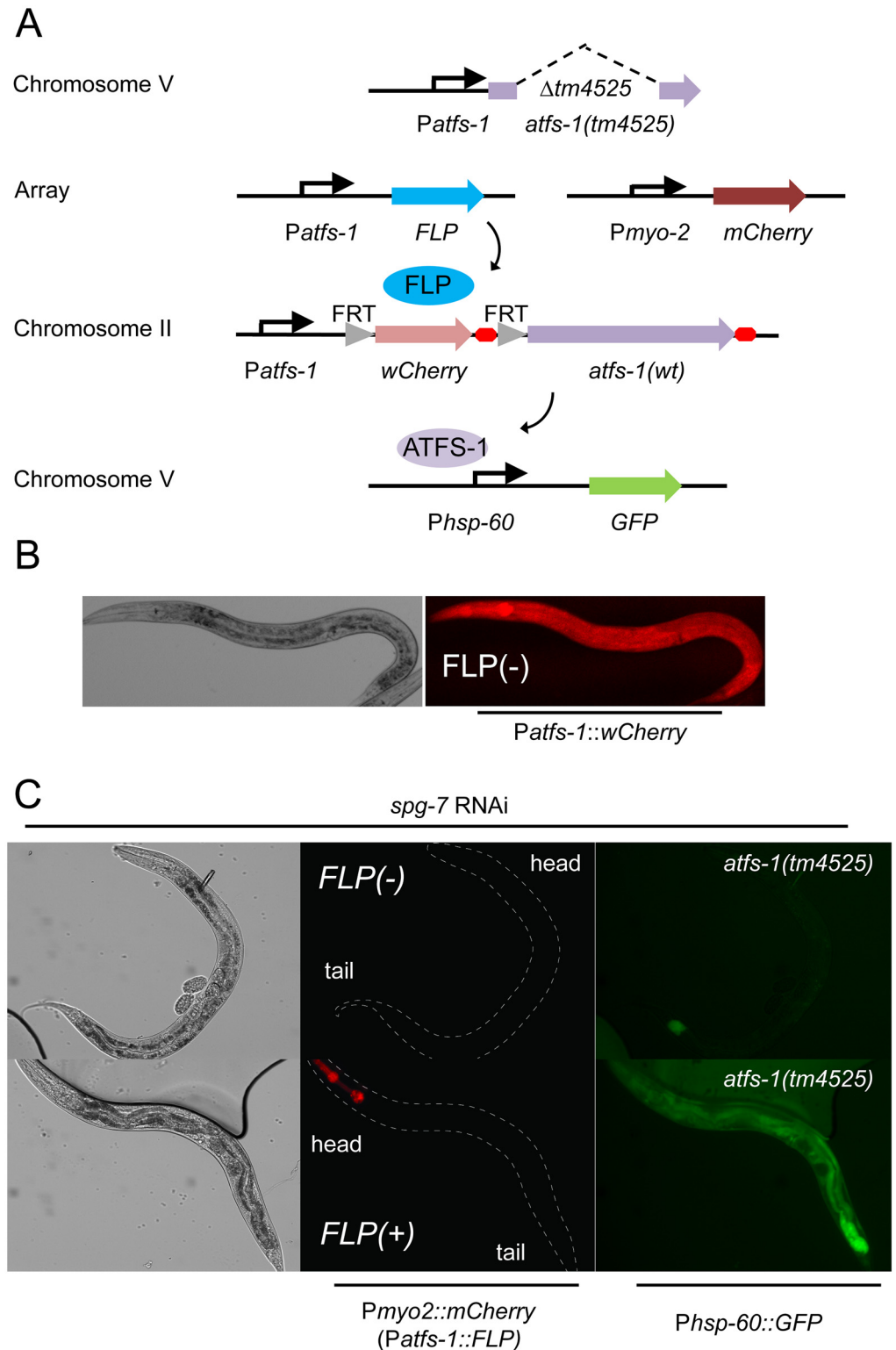
Fig 4. A FLP-out transgenic model to restrict UPR^mt activation. A.) Schematic showing relevant genetic constructs to restrict *atfs-1* expression using transgenic FLP recombinase and an *atfs-1* promoter interruption. The activity of the *flp* and *atfs-1* gene products on their target promoters is indicated by arrows. B.) Representative transmission and fluorescent photomicrographs of P*atfs-1*::*wCherry* expressed from a MosSCI single-copy, integrated *atfs-1* promoter interruption in the absence of FLP recombinase. C-E.) Photomicrographs

of DIC (grayscale), a fluorescent marker of transgenic FLP (red) and UPR^mt reporter P*hsp-60*::*GFP* (green) in *flp* (-) and F-H.) *flp(+)* siblings following *spg-7(RNAi)*. The genomic background is *atfs-1(tm4525)*, a loss-of-function allele.

In an attempt to discern regulated trafficking of the ATFS-1 transcription factor, a translational GFP fusion was expressed in the MosSCI system, but there was no detectable fluorescent signal even under conditions where we expected to observe increased nuclear trafficking ([S3 Fig](#)). We hypothesize that this is likely due to single copy gene expression and the presumed basal degradation of ATFS-1, as its physiologic effects in the nucleus are clearly observed ([Fig 4C](#)).

Next, the *atfs-1(et15)* gf missense mutation was incorporated into the MosSCI transgene, to generate a cell-specific compensatory response in the absence of stress. When FLP recombinase was expressed using the pan-neural promoter *rab-3* ([Fig 5A](#)), we observed robust activation of the UPR^mt *hsp-60*::*GFP* reporter gene in neurons ([Fig 5C–5H](#)). We predicted that remote activation of the UPR^mt would require *atfs-1* acting in distal tissues, and so we expressed the MosSCI/FLP transgene in a genomic *atfs-1(lf)* mutant background as a presumed negative control. However, we found that regardless of whether the MosSCI *atfs-1(gf)* transgene was in a genomic *atfs-1(lf)* or *atfs-1(+)* background, the UPR^mt was not activated in distal tissues ([Fig 5E and 5H](#)). The lack of remote UPR^mt activation in our model was not due to an inability of distal tissues to sense mitochondrial proteostasis, as they responded normally to EtBr ([S2](#) and [S3](#) Figs). Hence, restricted expression of ATFS-1(gf) can elicit a cell-autonomous UPR^mt, but cannot trigger its remote activation in other cells.

Finally, we asked whether the cell-autonomous UPR^mt activation observed in neurons reduced local A-R injury. The P*mec4*::mCherry reporter that was used to label mechanosensory neurons and their processes fluoresced much more brightly than the low level *wCherry* expressed from the single-copy promoter interruption ([Fig 6B](#)). We found that mechanosensory neurons from worms that exhibited FLP-mediated UPR^mt reporter activation ([Fig 6A](#)) were protected against axonal damage compared to their non-transgenic brood mates (*flp* null 2.6 ± 1.1; P*rab-3:flp* 1.7 ± 0.9, error is the SD, p = 0.04; [Fig 6D](#)). However, lethality following A-R was not influenced by the presence of the FLP transgene and did not correspond to UPR^mt reporter activation in neurons (*atfs-1(+)* background: *flp* null 73 ± 11%, P*rab-3:flp* 69 ± 13%, error is SEM, p = 0.69; [Fig 6E](#)). These results coincide with the lack of remote activation of the UPR^mt reporter ([Fig 5E and 5H](#); [S2 Fig](#)), and hence, we hypothesize that neuronal mitochondrial stress itself is required to synchronize adaptive responses in other tissues.

Discussion

It is clear from our results that pharmacologic or genetic pre-activation of the UPR^mt protects against 1.) A-R toxicity and 2.) axonal degeneration in neurons subject to sub-lethal A-R. We also find that mitochondrial dysfunction elicited through RNAi targeting of the ETC complex IV subunit *cco-1* in neurons can coordinate stress responses remotely to decrease A-R toxicity. Somewhat surprisingly however, neuronal expression of an *atfs-1(gf)* mutant did not reduce death, although it did function intrinsically to protect neurons themselves from axonal damage. Our results suggest that neuronal survival is not the major determinant of A-R survival and that *de facto* mitochondrial stress is required to coordinate remote stress responses through an unknown signal(s). However, our results do not discount a role for *atfs-1* acting in parallel to this unidentified signal, or being required in the target tissues independent of the signaling tissue. It's interesting that the homeodomain-containing transcription factor DVE-1 and the small ubiquitin-like protein UBL-5 are both encoded by genes required for signaling the
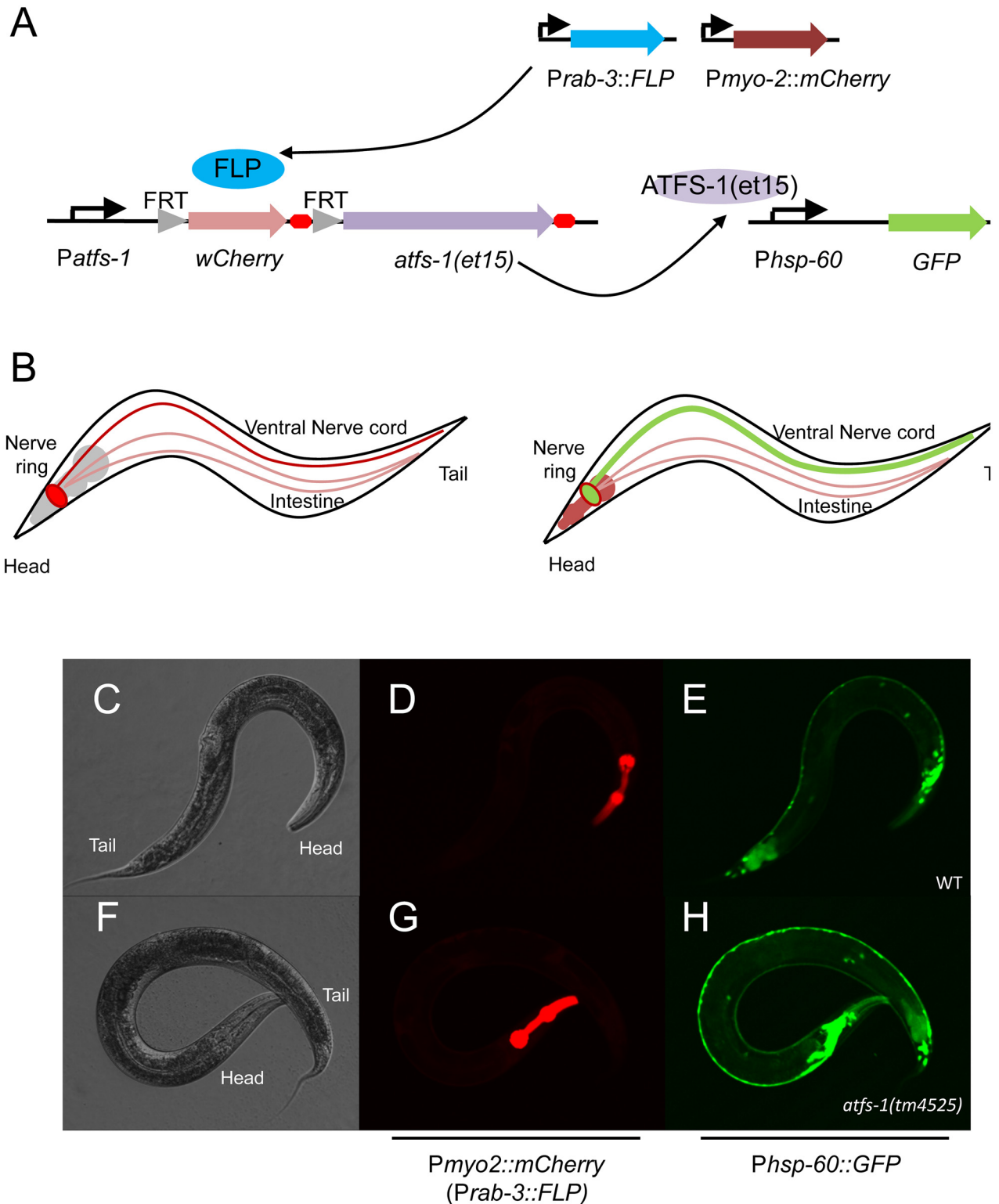
Fig 5. FLP-out *atfs-1(gf)* and trans-cellular UPR^mt signaling. A.) Schematic showing the relevant genetic constructs and the activity of the *flp* and *atfs-1* gene products on their target promoters. B.) Schematic representing UPR^mt activation in neurons (green) in the presence of P*rab-3*::*FLP* (red). The intestine is denoted in pink, as labeled, and activation of the UPR^mt is notably absent in this tissue. C-E.) Transmission and fluorescent photomicrographs of cell-autonomous UPR^mt activation in a genomic *atfs-1(+)* background and in a F-H.) *atfs-1(4525)* background. Note that distal tissues do not express the P*hsp-60*::*GFP* transgene, regardless of genetic background.

doi:10.1371/journal.pone.0159989.g005
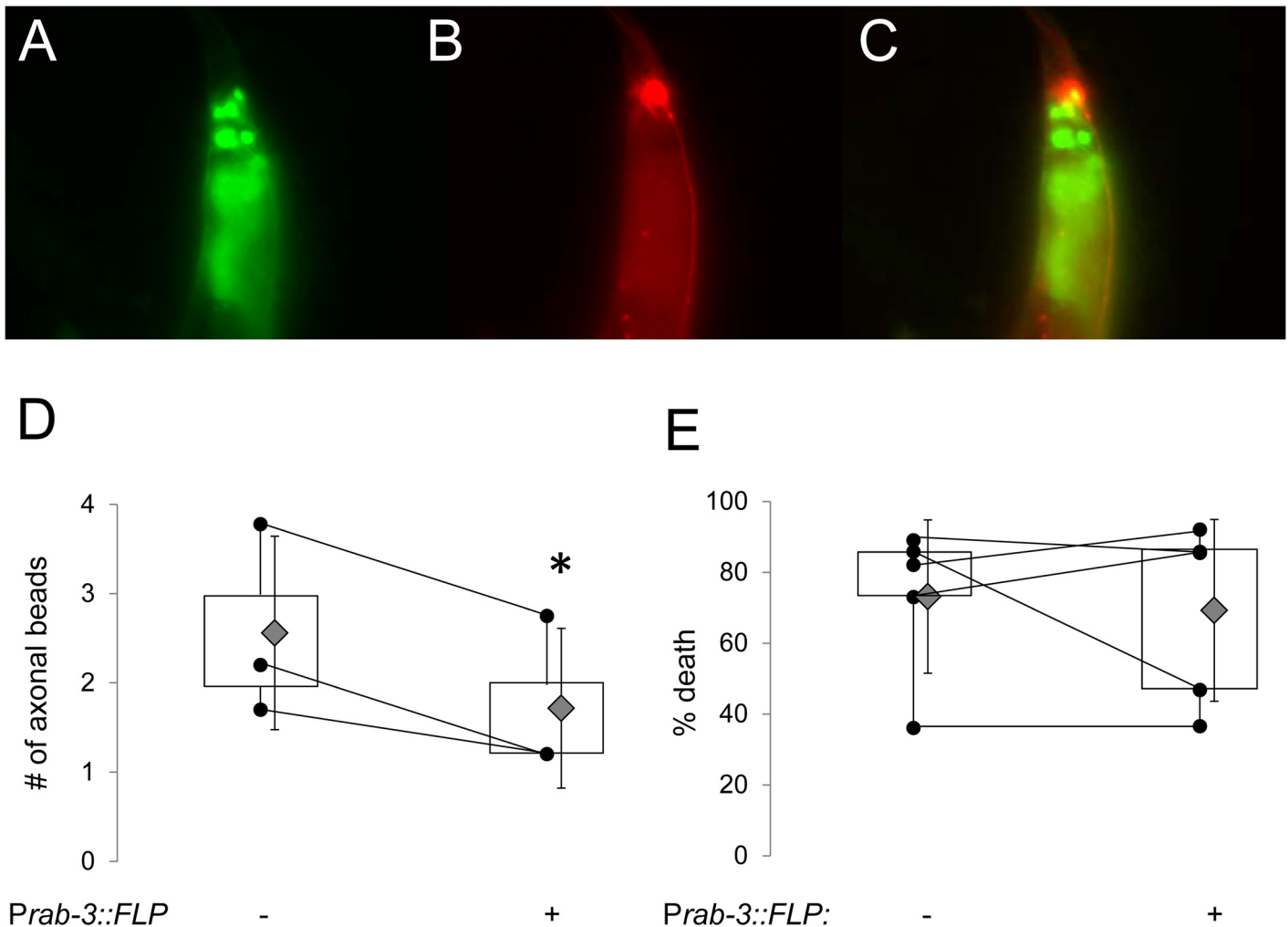
[Fig 6]. **Protecting neurons from local anoxia-reperfusion injury in the *atfs-1(gf)* FLP out worm does not reduce A-R death.** Representative fluorescent photomicrographs of a FLP out *atfs-1(et15)* transgenic worm with neuronal FLP (P*rab-3*::*FLP*) expressing A.) the UPR[mt] reporter P*hsp60*::*GFP* (green) and B.) the neuronal reporter P*mec-4*::*mCherry* in mechanosensory neurons. Labeling of the PLM cell processes can be clearly distinguished over background P*atfs-1*::*wCherry* from the un-excised promoter interruption in other cells. C.) Merge indicating co-localization of UPR[mt] activation and P*mec-4*::*mCherry*. D.) Expression of the FLP out *atfs-1(et15)* MosSCI transgene attenuates axonal damage following A-R (n = 3 independent trials of ~10 worms per genotype per trial), p*[Student's t test] <0.05). The error is the standard deviation. E.) Box-and-whisker plot indicating that neuronal FLP out *atfs-1(et15)* MosSCI transgene does not reduce death following A-R (n = 5, p*[Student's t test] <0.05). All data was obtained in an *atfs-1(+)* genomic background. Experimental replicates are shown as black dots; lines between replicates indicate that they were run on the same day. Grey diamonds are means with the error shown as standard deviations.

doi:10.1371/journal.pone.0159989.g006

UPR[mt] [3] and have been shown to work in parallel to *atfs-1*. In addition, mitochondrial function has been shown to regulate mTORC1 via ROS signaling (for review, see reference [45]), which together with its well established sensitivity to ATP may be central for metabolic adaptation and anoxic resistance and could potentially intertwine with UPR[mt] signaling.

The UPR[mt] has been suggested to be a surveillance response, whereby interruptions in core physiologic processes such as ETC function coordinate adaptation throughout the organism [12]. It seems intuitive that surveillance would best be served by a sentinel that's selectively vulnerable to the type of damage that's being detected (ie. a "first responder"). We speculate here that UPR[mt] activation in the germline (or stem cells?) may act as a sentinel for mitochondrial damage. Ethidium bromide, which causes mitochondrial stress and induces the UPR[mt], has

been shown to preferentially affect germline maintenance in *C. elegans*. There are multiple precedents for germline-soma signaling. For example, translation (like mitochondrial function) is monitored as a surveillance mechanism [11], and lipid signals generated from the germline in response to translation inhibition can induce stress signaling in distal tissues [13]. The germline is well recognized to generate signals that lead to metabolic remodeling of somatic tissues [46–48]. Within this context, it's quite interesting that stem cell maintenance also requires a UPR^mt mediated metabolic checkpoint [49]. Finally, we note that a previous report has shown that *glp-1* mutants which do not generate oocytes have altered fat stores and are greatly protected from A-R [50].

Genetic manipulations that impair mitochondrial function in *C. elegans* also alter lifespan [51]. Similarly, interventions that support protein folding are generally protective against low oxygen conditions and also extend lifespan [52]. One common denominator in these processes is that they rely on mitochondrial ROS in one capacity or another. However, an important difference is highlighted by recent work indicating that *atfs-1* is dispensable for *cco-1* RNAi mediated longevity [53]. In contrast, our work and that of others [27] indicate that protection from A-R injury via the UPR^mt requires *atfs-1* and, at least cell autonomously, that an ATFS-1(gf) that favors nuclear targeting is sufficient to reduce A-R death. Undoubtedly there are multiple signaling pathways that respond to mitochondrial stress, and the genetic requirements for protection from stress may overlap, but are likely to have insult specific components.

The UPR^mt like other compartment specific unfolded protein responses is aimed at restoring proteostasis in the face of stress. A general concept that emerges from multiple studies of stress is that adaptive signaling is generally beneficial in the short term, but chronic activation of these pathways is maladaptive. However, it's still unclear whether this holds true for the UPR^mt. For example, it's been established that pre-activation of the UPR^mt protects against statin toxicity [42] and *Pseudomonas* infection [10]. In addition, several *C. elegans* mutants in electron transport chain (ETC) subunits require *atfs-1* for survival [16], suggesting that at least within the context of mitochondrial dysfunction any potential drawbacks of chronic activation are outweighed by the benefits. So, can we conclude that the UPR^mt is strictly beneficial?

Unfortunately, there are several observations suggesting that this is not as straightforward as would appear, and probably depends upon the degree of activation. Treatment with *spg-7 (RNAi)* can cause larval maturation to stall, as can high concentrations of EtBr, both of which are means of activating the UPR^mt. One might argue that these phenotypes result from excess mitochondrial dysfunction that cannot be compensated for by activation of the UPR^mt. However, it is worth noting that the *atfs-1(et15)* gf mutant is generally smaller and matures more slowly than wildtype worms and displays reduced fecundity [42]. In addition, worms expressing an a nuclear targeted ATFS-1 with a deletion of the mitochondrial targeting sequence(Δ1-32.myc ATFS-1) similarly develop slower than worms expressing a wildtype ATFS-1 [16]. This may result from chronic nuclear activation, or alternatively from reduced ATFS-1 function in the mitochondria, whose genome has also been shown to be regulated by this transcription factor [15]. Hence, while there's reason to believe that the UPR^mt may be primarily beneficial, further work is required to delineate the downside of chronic activation.

Collectively, our results demonstrate that *atfs-1* and the UPR^mt can influence A-R damage and survival. We further hypothesize that mitochondrial stress activates an as-of-yet unidentified signaling pathway(s) to coordinate adaptive responses throughout the organism. While the mammalian ATFS-1 ortholog has yet to be identified, the similarities between the UPR^mt in mammals and worms (for review, see reference [54] and the strong protection from A-R elicited by activation of the UPR^mt warrant further work on this topic.

Supporting Information

S1 Fig. UPR^{mt} activation by ethidium bromide reduces death following anoxia-reperfusion and requires *atfs-1*. A.) Box-and-whisker plot of A-R toxicity following treatment with 30 μg/ml EtBr to activate the UPR^{mt} (n = 8, p*[Student's t test] <0.05) B.) *atfs-1(tm4525)* mutants fail to exhibit EtBr mediated protection (n = 5, p*[Student's t test] <0.05). Grey diamonds are means with the error shown as standard deviations.
(PDF)

S2 Fig. Distal tissues are capable of mounting an UPR^{mt} in the neuron specific *atfs-1(gf)* FLP-out transgenic model. Representative fluorescent photomicrographs of MosSCI FLP-out *atfs-1(gf)* transgenic worms grown on (A, C.) control plates and (B, D.) plates containing 30μg/mL EtBr. The transgenic marker for FLP (P*myo-2::mCherry*) is shown in panels A and B, while activation of the UPR^{mt} reporter P*hsp-60*::GFP is shown in panels C and D. The genomic background is *atfs-1(+)*. These data indicate that failure to activate distal tissue stress responses in this strain does not result from an intrinsic dysfunction.
(PDF)

S3 Fig. Distal tissues remain responsive to UPR^{mt} inducers in the neuron specific FLP-out transgenic model. Representative photomicrographs of MosSCI FLP-out *atfs-1(gf)* transgenic worms grown on (A, C, F, H.) control plates and (B, D, E, G, I, J) plates containing 30μg/mL EtBr. Transmitted light images are shown in panels A-E, while fluorescent images are shown in panels F-J. Relevant information is labeled at the top of the figure. Note that the strain in panels E and J lacks the UPR^{mt} reporter P*hsp-60*::GFP and that the MosSCI FLP-out *atfs-1(gf)* is fused to GFP. These panels have been overexposed. The failure to detect either mitochondrial or nuclear GFP (the green is autofluorescence) exemplifies the low expression level of a single copy transgene and its likely degradation under basal conditions.
(PDF)

S1 Table. Raw data. This is an Excel spreadsheet with the raw data organized by figure. Technical and experimental replicates are indicated.
(XLSX)

Author Contributions

Conceived and designed the experiments: SP TS PSB KN. Performed the experiments: SP TS. Analyzed the data: SP TS KN. Wrote the paper: SP KN.

References

1. Zhao Q, Wang J, Levichkin IV, Stasinopoulos S, Ryan MT, Hoogenraad NJ. A mitochondrial specific stress response in mammalian cells. The EMBO journal. 2002; 21(17):4411–9. Epub 2002/08/29. PMID: 12198143; PubMed Central PMCID: PMC126185.

2. Benedetti C, Haynes CM, Yang Y, Harding HP, Ron D. Ubiquitin-like protein 5 positively regulates chaperone gene expression in the mitochondrial unfolded protein response. Genetics. 2006; 174(1):229–39. doi: 10.1534/genetics.106.061580 PMID: 16816413; PubMed Central PMCID: PMC1569816.

3. Haynes CM, Petrova K, Benedetti C, Yang Y, Ron D. ClpP mediates activation of a mitochondrial unfolded protein response in C. elegans. Developmental cell. 2007; 13(4):467–80. Epub 2007/10/11. doi: 10.1016/j.devcel.2007.07.016 PMID: 17925224.

4. Haynes CM, Yang Y, Blais SP, Neubert TA, Ron D. The matrix peptide exporter HAF-1 signals a mitochondrial UPR by activating the transcription factor ZC376.7 in C. elegans. Molecular cell. 2010; 37 (4):529–40. doi: 10.1016/j.molcel.2010.01.015 PMID: 20188671; PubMed Central PMCID: PMC2846537.

5. Yoneda T, Benedetti C, Urano F, Clark SG, Harding HP, Ron D. Compartment-specific perturbation of protein handling activates genes encoding mitochondrial chaperones. Journal of cell science. 2004; 117(Pt 18):4055–66. doi: 10.1242/jcs.01275 PMID: 15280428.

6. Lin YF, Haynes CM. Metabolism and the UPR(mt). Molecular cell. 2016; 61(5):677–82. doi: 10.1016/j. molcel.2016.02.004 PMID: 26942672; PubMed Central PMCID: PMC4779188.

7. Houtkooper RH, Mouchiroud L, Ryu D, Moullan N, Katsyuba E, Knott G, et al. Mitonuclear protein imbalance as a conserved longevity mechanism. Nature. 2013; 497(7450):451–7. Epub 2013/05/24. doi: 10.1038/nature12188 PMID: 23698443; PubMed Central PMCID: PMC3663447.

8. Runkel ED, Liu S, Baumeister R, Schulze E. Surveillance-activated defenses block the ROS-induced mitochondrial unfolded protein response. PLoS genetics. 2013; 9(3):e1003346. doi: 10.1371/journal. pgen.1003346 PMID: 23516373; PubMed Central PMCID: PMC3597513.

9. Rauthan M, Ranji P, Abukar R, Pilon M. A Mutation in Caenorhabditis elegans NDUF-7 Activates the Mitochondrial Stress Response and Prolongs Lifespan via ROS and CED-4. G3. 2015; 5(8):1639–48. doi: 10.1534/g3.115.018598 PMID: 26038366; PubMed Central PMCID: PMC4528320.

10. Pellegrino MW, Nargund AM, Kirienko NV, Gillis R, Fiorese CJ, Haynes CM. Mitochondrial UPR-regulated innate immunity provides resistance to pathogen infection. Nature. 2014; 516(7531):414–7. doi: 10.1038/nature13818 PMID: 25274306; PubMed Central PMCID: PMC4270954.

11. Dunbar TL, Yan Z, Balla KM, Smelkinson MG, Troemel ER. C. elegans detects pathogen-induced translational inhibition to activate immune signaling. Cell host & microbe. 2012; 11(4):375–86. doi: 10. 1016/j.chom.2012.02.008 PMID: 22520465; PubMed Central PMCID: PMC3334869.

12. Liu Y, Samuel BS, Breen PC, Ruvkun G. Caenorhabditis elegans pathways that surveil and defend mitochondria. Nature. 2014; 508(7496):406–10. doi: 10.1038/nature13204 PMID: 24695221; PubMed Central PMCID: PMC4102179.

13. Govindan JA, Jayamani E, Zhang X, Breen P, Larkins-Ford J, Mylonakis E, et al. Lipid signalling couples translational surveillance to systemic detoxification in Caenorhabditis elegans. Nature cell biology. 2015; 17(10):1294–303. doi: 10.1038/ncb3229 PMID: 26322678; PubMed Central PMCID: PMC4589496.

14. Durieux J, Wolff S, Dillin A. The cell-non-autonomous nature of electron transport chain-mediated longevity. Cell. 2011; 144(1):79–91. doi: 10.1016/j.cell.2010.12.016 PMID: 21215371; PubMed Central PMCID: PMC3062502.

15. Nargund AM, Fiorese CJ, Pellegrino MW, Deng P, Haynes CM. Mitochondrial and nuclear accumulation of the transcription factor ATFS-1 promotes OXPHOS recovery during the UPR(mt). Molecular cell. 2015; 58(1):123–33. doi: 10.1016/j.molcel.2015.02.008 PMID: 25773600; PubMed Central PMCID: PMC4385436.

16. Nargund AM, Pellegrino MW, Fiorese CJ, Baker BM, Haynes CM. Mitochondrial import efficiency of ATFS-1 regulates mitochondrial UPR activation. Science. 2012; 337(6094):587–90. doi: 10.1126/ science.1223560 PMID: 22700657; PubMed Central PMCID: PMC3518298.

17. Murphy E, Steenbergen C. Mechanisms underlying acute protection from cardiac ischemia-reperfusion injury. Physiological reviews. 2008; 88(2):581–609. doi: 10.1152/physrev.00024.2007 PMID: 18391174; PubMed Central PMCID: PMC3199571.

18. Hardy DL, Clark JB, Darley-Usmar VM, Smith DR. Reoxygenation of the hypoxic myocardium causes a mitochondrial complex I defect. Biochemical Society transactions. 1990; 18(4):549. PMID: 1703502.

19. Asimakis GK, Conti VR. Myocardial ischemia: correlation of mitochondrial adenine nucleotide and respiratory function. Journal of molecular and cellular cardiology. 1984; 16(5):439–47. PMID: 6737484.

20. Brookes PS, Yoon Y, Robotham JL, Anders MW, Sheu SS. Calcium, ATP, and ROS: a mitochondrial love-hate triangle. American journal of physiology Cell physiology. 2004; 287(4):C817–33. doi: 10. 1152/ajpcell.00139.2004 PMID: 15355853.

21. Borutaite V, Mildaziene V, Brown GC, Brand MD. Control and kinetic analysis of ischemia-damaged heart mitochondria: which parts of the oxidative phosphorylation system are affected by ischemia? Biochimica et biophysica acta. 1995; 1272(3):154–8. PMID: 8541346.

22. Garcia-Rivas Gde J, Carvajal K, Correa F, Zazueta C. Ru360, a specific mitochondrial calcium uptake inhibitor, improves cardiac post-ischaemic functional recovery in rats in vivo. British journal of

pharmacology. 2006; 149(7):829–37. doi: 10.1038/sj.bjp.0706932 PMID: 17031386; PubMed Central PMCID: PMC2014682.

23. Paradies G, Ruggiero FM, Petrosillo G, Quagliariello E. Peroxidative damage to cardiac mitochondria: cytochrome oxidase and cardiolipin alterations. FEBS letters. 1998; 424(3):155–8. PMID: 9539141.

24. Horwitz LD, Fennessey PV, Shikes RH, Kong Y. Marked reduction in myocardial infarct size due to prolonged infusion of an antioxidant during reperfusion. Circulation. 1994; 89(4):1792–801. PMID: 8149545.

25. Piot C, Croisille P, Staat P, Thibault H, Rioufol G, Mewton N, et al. Effect of cyclosporine on reperfusion injury in acute myocardial infarction. The New England journal of medicine. 2008; 359(5):473–81. doi: 10.1056/NEJMoa071142 PMID: 18669426.

26. Argaud L, Gateau-Roesch O, Muntean D, Chalabreysse L, Loufouat J, Robert D, et al. Specific inhibition of the mitochondrial permeability transition prevents lethal reperfusion injury. Journal of molecular and cellular cardiology. 2005; 38(2):367–74. PMID: 15698843.

27. Kaufman DM, Crowder CM. Mitochondrial Proteostatic Collapse Leads to Hypoxic Injury. Current biology: CB. 2015; 25(16):2171–6. doi: 10.1016/j.cub.2015.06.062 PMID: 26234215.

28. Van Voorhies WA, Ward S. Broad oxygen tolerance in the nematode Caenorhabditis elegans. The Journal of experimental biology. 2000; 203(Pt 16):2467–78. PMID: 10903161.

29. Belke DD, Gloss B, Hollander JM, Swanson EA, Duplain H, Dillmann WH. In vivo gene delivery of HSP70i by adenovirus and adeno-associated virus preserves contractile function in mouse heart following ischemia-reperfusion. American journal of physiology Heart and circulatory physiology. 2006; 291(6):H2905–10. doi: 10.1152/ajpheart.00323.2006 PMID: 16920815.

30. Lin KM, Lin B, Lian IY, Mestril R, Scheffler IE, Dillmann WH. Combined and individual mitochondrial HSP60 and HSP10 expression in cardiac myocytes protects mitochondrial function and prevents apoptotic cell deaths induced by simulated ischemia-reoxygenation. Circulation. 2001; 103(13):1787–92. Epub 2001/04/03. PMID: 11282911.

31. Anderson LL, Mao X, Scott BA, Crowder CM. Survival from hypoxia in C. elegans by inactivation of aminoacyl-tRNA synthetases. Science. 2009; 323(5914):630–3. Epub 2009/01/31. doi: 10.1126/science.1166175 PMID: 19179530.

32. Stiernagle T. Maintenance of C. elegans. WormBook: the online review of C elegans biology. 2006:1–11. doi: 10.1895/wormbook.1.101.1 PMID: 18050451; PubMed Central PMCID: PMC4781397.

33. Frokjaer-Jensen C, Davis MW, Hopkins CE, Newman BJ, Thummel JM, Olesen SP, et al. Single-copy insertion of transgenes in Caenorhabditis elegans. Nature genetics. 2008; 40(11):1375–83. doi: 10.1038/ng.248 PMID: 18953339; PubMed Central PMCID: PMC2749959.

34. Hagen FK, Nehrke K. cDNA cloning and expression of a family of UDP-N-acetyl-D-galactosamine:polypeptide N-acetylgalactosaminyltransferase sequence homologs from Caenorhabditis elegans. The Journal of biological chemistry. 1998; 273(14):8268–77. PMID: 9525933.

35. Rieckher M, Kourtis N, Pasparaki A, Tavernarakis N. Transgenesis in Caenorhabditis elegans. Methods in molecular biology. 2009; 561:21–39. doi: 10.1007/978-1-60327-019-9_2 PMID: 19504062.

36. Frokjaer-Jensen C, Davis MW, Ailion M, Jorgensen EM. Improved Mos1-mediated transgenesis in C. elegans. Nature methods. 2012; 9(2):117–8. doi: 10.1038/nmeth.1865 PMID: 22290181; PubMed Central PMCID: PMC3725292.

37. Wojtovich AP, DiStefano P, Sherman T, Brookes PS, Nehrke K. Mitochondrial ATP-sensitive potassium channel activity and hypoxic preconditioning are independent of an inwardly rectifying potassium channel subunit in Caenorhabditis elegans. FEBS letters. 2012; 586(4):428–34. doi: 10.1016/j.febslet.2012.01.021 PMID: 22281198; PubMed Central PMCID: PMC3288502.

38. Scott BA, Avidan MS, Crowder CM. Regulation of hypoxic death in C. elegans by the insulin/IGF receptor homolog DAF-2. Science. 2002; 296(5577):2388–91. Epub 2002/06/18. doi: 10.1126/science.1072302 PMID: 12065745.

39. Queliconi BB, Marazzi TB, Vaz SM, Brookes PS, Nehrke K, Augusto O, et al. Bicarbonate modulates oxidative and functional damage in ischemia-reperfusion. Free radical biology & medicine. 2013; 55:46–53. doi: 10.1016/j.freeradbiomed.2012.11.007 PMID: 23195687; PubMed Central PMCID: PMC3995138.

40. Padilla PA, Nystul TG, Zager RA, Johnson AC, Roth MB. Dephosphorylation of cell cycle-regulated proteins correlates with anoxia-induced suspended animation in Caenorhabditis elegans. Molecular biology of the cell. 2002; 13(5):1473–83. doi: 10.1091/mbc.01-12-0594 PMID: 12006646; PubMed Central PMCID: PMC111120.

41. Rodriguez M, Snoek LB, De Bono M, Kammenga JE. Worms under stress: C. elegans stress response and its relevance to complex human disease and aging. Trends in genetics: TIG. 2013; 29(6):367–74. doi: 10.1016/j.tig.2013.01.010 PMID: 23428113.

42. Rauthan M, Ranji P, Aguilera Pradenas N, Pitot C, Pilon M. The mitochondrial unfolded protein response activator ATFS-1 protects cells from inhibition of the mevalonate pathway. Proceedings of the National Academy of Sciences of the United States of America. 2013; 110(15):5981–6. doi: 10.1073/pnas.1218778110 PMID: 23530189; PubMed Central PMCID: PMC3625262.

43. Pinan-Lucarre B, Gabel CV, Reina CP, Hulme SE, Shevkoplyas SS, Slone RD, et al. The core apoptotic executioner proteins CED-3 and CED-4 promote initiation of neuronal regeneration in Caenorhabditis elegans. PLoS biology. 2012; 10(5):e1001331. doi: 10.1371/journal.pbio.1001331 PMID: 22629231; PubMed Central PMCID: PMC3358320.

44. Davis MW, Morton JJ, Carroll D, Jorgensen EM. Gene activation using FLP recombinase in C. elegans. PLoS genetics. 2008; 4(3):e1000028. doi: 10.1371/journal.pgen.1000028 PMID: 18369447; PubMed Central PMCID: PMC2265415.

45. Groenewoud MJ, Zwartkruis FJ. Rheb and mammalian target of rapamycin in mitochondrial homoeostasis. Open biology. 2013; 3(12):130185. doi: 10.1098/rsob.130185 PMID: 24352740; PubMed Central PMCID: PMC3877845.

46. Tsang WY, Lemire BD. Mitochondrial genome content is regulated during nematode development. Biochemical and biophysical research communications. 2002; 291(1):8–16. doi: 10.1006/bbrc.2002.6394 PMID: 11829454.

47. Ratnappan R, Amrit FR, Chen SW, Gill H, Holden K, Ward J, et al. Germline signals deploy NHR-49 to modulate fatty-acid beta-oxidation and desaturation in somatic tissues of C. elegans. PLoS genetics. 2014; 10(12):e1004829. doi: 10.1371/journal.pgen.1004829 PMID: 25474470; PubMed Central PMCID: PMC4256272.

48. Wang MC, O'Rourke EJ, Ruvkun G. Fat metabolism links germline stem cells and longevity in C. elegans. Science. 2008; 322(5903):957–60. doi: 10.1126/science.1162011 PMID: 18988854; PubMed Central PMCID: PMC2760269.

49. Mohrin M, Shin J, Liu Y, Brown K, Luo H, Xi Y, et al. Stem cell aging. A mitochondrial UPR-mediated metabolic checkpoint regulates hematopoietic stem cell aging. Science. 2015; 347(6228):1374–7. doi: 10.1126/science.aaa2361 PMID: 25792330; PubMed Central PMCID: PMC4447312.

50. Mendenhall AR, LeBlanc MG, Mohan DP, Padilla PA. Reduction in ovulation or male sex phenotype increases long-term anoxia survival in a daf-16-independent manner in Caenorhabditis elegans. Physiological genomics. 2009; 36(3):167–78. doi: 10.1152/physiolgenomics.90278.2008 PMID: 19050081; PubMed Central PMCID: PMC2646460.

51. Dillin A, Hsu AL, Arantes-Oliveira N, Lehrer-Graiwer J, Hsin H, Fraser AG, et al. Rates of behavior and aging specified by mitochondrial function during development. Science. 2002; 298(5602):2398–401. doi: 10.1126/science.1077780 PMID: 12471266.

52. Mabon ME, Mao X, Jiao Y, Scott BA, Crowder CM. Systematic identification of gene activities promoting hypoxic death. Genetics. 2009; 181(2):483–96. doi: 10.1534/genetics.108.097188 PMID: 19047414; PubMed Central PMCID: PMC2644942.

53. Bennett CF, Vander Wende H, Simko M, Klum S, Barfield S, Choi H, et al. Activation of the mitochondrial unfolded protein response does not predict longevity in Caenorhabditis elegans. Nature communications. 2014; 5:3483. doi: 10.1038/ncomms4483 PMID: 24662282; PubMed Central PMCID: PMC3984390.

54. Arnould T, Michel S, Renard P. Mitochondria Retrograde Signaling and the UPR mt: Where Are We in Mammals? International journal of molecular sciences. 2015; 16(8):18224–51. doi: 10.3390/ijms160818224 PMID: 26258774; PubMed Central PMCID: PMC4581242.